3 Surfaces and Interfaces

3-1 Adsorption Site and Three-Dimensional Structure of Ni Atoms on TiO_2(110) Determined by Polarization-Dependent Total-Reflection Fluorescence EXAFS

Identifying the precise adsorption site of metal species on metal oxide surfaces is the first step towards understanding the metal-oxide interactions which govern the characteristic properties of catalysts, sensors, photocatalysts and fuel cells. Scanning-probe microscopy can provide information on the morphology and size of metal species on metal oxide surfaces. However, it is difficult to identify individual chemical species and determine bond features precisely. On the other hand, the polarization-dependent total-reflection fluorescence EXAFS (PTRF-EXAFS) technique can be used to determine accurate three-dimensional surface structures of overlayer metals interacting with substrate surfaces at sub-Ångstrom resolution [1-5]. In this work we have used the PTRF-EXAFS technique to determine the adsorption site and three-dimensional structure of Ni atoms on a TiO_2(110) surface as a model for supported Ni catalysts active for CO or alkene hydrogenation.

A clean TiO_2(110) (1 × 1) surface was prepared by several cycles of Ar^+ sputtering at room temperature and annealing at 873 K. Ni was evaporated by resistively heating a tungsten filament wrapped with a Ni wire. By considering the surface structure of TiO_2(110) (Fig. 1), PTRF-EXAFS measurements were carried out at BL-9A with three different orientations of the electric vector ($\vec{E}$) of the incident X-rays with respect to the surface; two parallel orientations $\vec{E}$ // [001] and [1$\bar{1}$0], and the perpendicular orientation $\vec{E}$ // [110]. Ni Kα fluorescence was detected with a 19-element Ge solid state detector. An EXAFS analysis was carried out using the REX 2000 [6] and FEFF8.02 codes [7].

Figure 2 (a) shows the Ni K-edge PTRF-EXAFS spectra observed with a coverage of 1 × 10^{13} atoms/cm^2. The amplitude of all observed EXAFS spectra decays quickly with *k*. The results indicate that the nearest neighbors of Ni can be oxygen atoms, and that the Ni atoms are atomically dispersed on the surface. To derive a definite adsorption structure an iterative method using the FEFF code and a real-space model structure

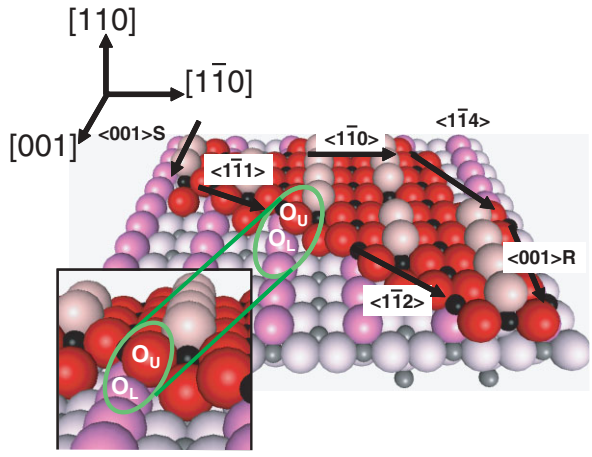

Figure 1
Structure of the TiO_2(110) (1 × 1) surface. The inset shows the<1$\bar{1}$n> step edge of the TiO_2(110) surface in detail. Smooth (<001>S) and rugged (<001>R) step edge structures are indicated.

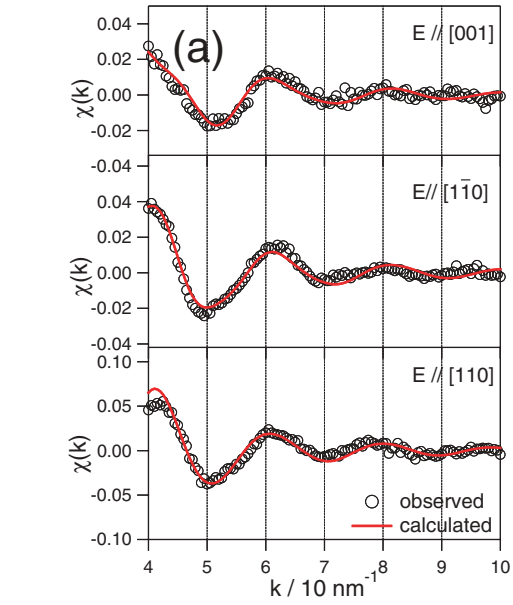

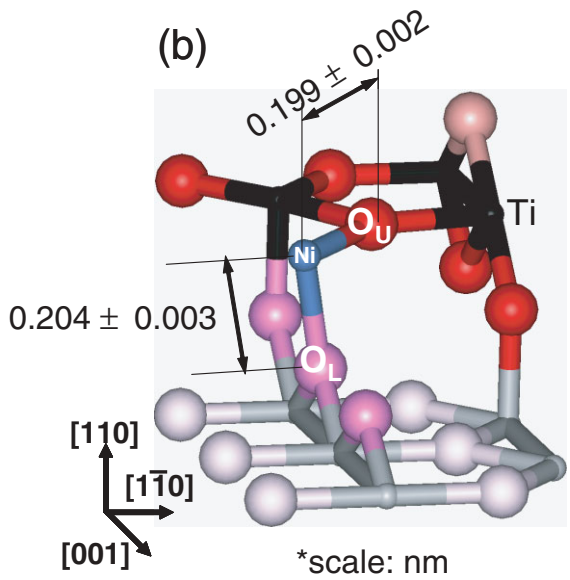

Figure 2
(a) Observed (black open circles) and calculated (red lines) PTRF-EXAFS spectra of Ni on TiO_2(110). (b) Proposed model structure of Ni atoms on TiO_2(110).

was employed [1-4]. This analysis shows that the stable adsorption sites of the Ni atoms were on the <1$\bar{1}$n> step edge of the TiO_2 (110) surface (shown in the inset of Fig. 1). The site consists of bridging oxygen atoms O on the lower terrace (O_L) and the upper terrace (O_U) (Fig. 2(b)). With a Ni atom located at this site the calculations reproduce well the observed spectra (Fig. 2(a)). The Ni-O_L and Ni-O_U distances were determined at 0.204 ± 0.003 nm and 0.199 ± 0.002 nm. Interestingly, the Ni adsorption site corresponds to the imaginary Ti site of the next TiO_2 layer growing from the step edge. Combined with our previous results that a Ni atom on Al_2O_3 (0001) is located at the imaginary Al site of the new Al_2O_3 layer [2], this new result suggests that the imaginary cation site above metal oxide surfaces should be the most stable site for metal atoms. In other words, metal atoms should be located at the sites to which the dangling bonds of the surface oxygen atoms are directed. Surface defects have often been recognized as important adsorption sites on metals and semiconductors. In this context, the oxygen defect (see the inset of Fig. 1) where Ti^{4+} is exposed can be assumed to play an important role for metal adsorption on the TiO_2 surface. This study clearly shows that the polarity of defects is significant for metal adsorption on oxide surfaces.

W. -J. Chun[1, 2], Y. Koike[3], K. Ijima[4], K. Fujikawa[1], Y. Iwasawa[5], M. Nomura[3] and K. Asakura[1] ([1]Hokkaido Univ., [2]JST-CREST, [3]KEK-PF, [4]Yamanashi Univ., [5]The Univ. of Tokyo)

References

[1] Y. Koike, K. Ijima, W. -J. Chun, H. Ashima, T. Yamamoto, K. Fujikawa, S. Suzuki, Y. Iwasawa, M. Nomura and K. Asakura, *Chem. Phys. Lett.*, **421** (2006) 27.
[2] K. Ijima, Y. Koike, W. -J. Chun, Y. Saito, Y. Tanizawa, T. Shido, Y. Iwasawa, M. Nomura and K. Asakura, *Chem. Phys. Lett.*, **384** (2004) 134.
[3] Y. Tanizawa, T. Shido, W. -J. Chun, K. Asakura, M. Nomura and Y. Iwasawa, *J. Phys. Chem. B*, **107** (2003) 12917.
[4] W. -J. Chun, K. Sakura and Y. Iwasawa, *J. Phys. Chem. B*, **102** (1998) 9006.
[5] K. Asakura, W. -J. Chun, M. Shirai, K. Tomishige and Y. Iwasawa, *J. Phys. Chem. B*, **101** (1997) 5549.
[6] EXAFS analysis program package coded by Rigaku Co. Japan.
[7] A. L. Ankudinov, B. Ravel, J. J. Rehr and S. D. Conradson, *Phys. Rev. B*, **58** (1998) 7565.

3-2 Strain Distribution at Buried Interfaces due to Ion Implantation Revealed by Extremely Asymmetric X-Ray Diffraction

Implantation of MeV ions occupies an important position in the field of semiconductor engineering, such as the fabrication of buried insulator layers, buried conducting layers, and VLSI deep wells. In this report, the surface strain of Si(111) surfaces implanted with 1.5-MeV Au^{2+} ions was observed using extremely asymmetric X-ray diffraction. A broad sub-peak accompanied by intensity oscillations was observed on the low-angle side of the bulk peak in the measured rocking curves. The lattice strain due to ion implantation was evaluated by fitting to a curve calculated using dynamical diffraction theory [1].

We have developed an “Extremely Asymmetric X-ray Diffraction” technique that uses asymmetric Bragg-case reflection under grazing incidence [1-3]. The technique is sensitive to the strain near the surface because the incident angle of the X-rays is set near to the critical angle of total reflection. The technique has been used to study the strain fields of SiO_2/Si interfaces [2] and Ni diffused Si surfaces [3].

Au^{2+} ions were implanted into Si(111) wafers at room temperature using the 3.0-MV pelletron accelerator facility at the Institute of Physics, Bhubaneswar, India. The kinetic energy of the ions was 1.5 MeV, and the implantation was carried up to a fluence of 5×10^{13} ions/cm^2 while keeping the incident ion current at 20 nA. The strain was observed at room temperature in the atmospheric environment at BL-15C. Rocking curves of the Si 113 reflection of the samples were recorded using X-ray beams of 0.16-nm wavelength at a grazing incident angle of ~0.2° with respect to the surface.

The blue open circles of Fig. 3 show the experimentally observed rocking curve. The fundamental characteristic of the rocking curve is a broad sub-peak accompanied by intensity oscillations on the low-angle side of the bulk peak. The existence of the low-angle side sub-peak indicates a distorted crystal layer with expanded lattice spacing of the (113) plane. The strain was evaluated by fitting the observed curve to curves calculated using dynamical diffraction theory [4]. For the simulation we assumed a strain distribution along the surface normal direction. The strain distribution function consists of two Fermi-Dirac functions given by:

$$\varepsilon(Z) = \frac{P_1}{1+\exp[-(P_2 - z)/P_3]} + \frac{P_1}{1+\exp[(P_4 - z)/P_5]} - P_1$$

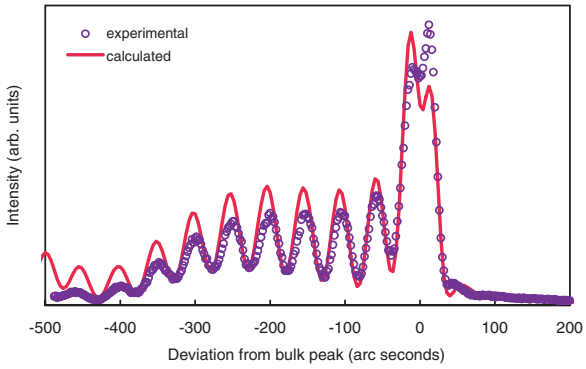

Figure 3
Experimentally observed Si 113 rocking curve (blue open circles) and the result of curve fitting (red line).

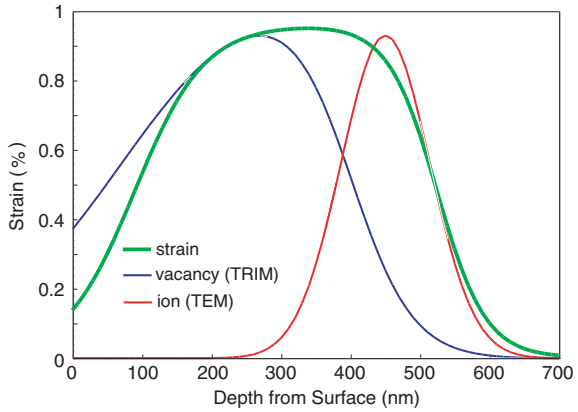

Figure 4
Resultant strain profile (green), the projected range of Au ion distribution evaluated from a TEM image (red), and the distribution of vacancies (blue) calculated using the TRIM code.

where z represents the depth from the surface, P_1 the maximum value of the strain, P_2 the position of the structural transition layer near the surface, P_3 the extent of the transition layer near the surface, P_4 the position of the structural transition layer in the bulk, and P_5 the extent of the transition layer in the bulk. Details of the simulation are reported elsewhere [1].

Figure 4 shows the resulting strain profiles (green thick curve), and the rocking curve calculated using these profiles is shown as the red curve in Fig. 3. It is clear that the (111) spacing expands by ~500 nm under the surface. For comparison, the projected range distribution of the implanted ions is displayed in Fig. 4 by a red curve. This distribution was evaluated from a cross-sectional transmission electron microscopy (TEM) image [1]. Comparison of the strain profile with the projected range distribution noticeably shows that the deep side of these curves agree with each other, indicating that the strain near the interface between the distorted layer and the bulk arises from Au ions occupying interstitial sites. On the other hand, the lattice distortion near the surface may originate from vacancies due to elastic collisions between target atoms and ions. A vacancy distribution curve was calculated uing the TRIM code [5], and is shown as a blue curve in Fig. 4. The result of the expansion of the (111) spacing indicates that recoiled Si atoms form self-interstitials near the surface.

In conclusion, it has been found that the lattice spacing of the (111) plane expanded by ~500 nm under the surface [1]. In addition, a simulation of rocking curves vs. strain parameters revealed that the present technique is sensitive to the strain profile within a depth of ~80 nm [1].

T. Emoto[1], P. V. Satyam[2] and K. Akimoto[3] ([1]Toyota National College of Tech., [2]Inst. of Phys., India, [3]Nagoya Univ.)

References

[1] T. Emoto, K. Akimoto, K. Ito, J. Ghatak and P. V. Satyam, *e-J. Surf. Sci. Nanotech.*, **4** (2006) 25.
[2] T. Emoto, K. Akimoto and A. Ichimiya, *Surf. Sci.*, **438** (1999) 107.
[3] T. Emoto, K. Akimoto, A. Ichimiya and K. Hirose, *Appl. Surf. Sci.*, **190** (2002) 113.
[4] T. Takahashi and S. Nakatani, *Surf. Sci.*, **326** (1995) 347.
[5] J. F. Ziegler, J. P. Biersack and U. Littmark, *The Stopping and Range of Ions in Solids*, Pergamon Press, New York, **Chap. 8**. (1985).

3-3 Surface State Created by Strain in Ge Nanoislands on a Si(111) Surface

Germanium quantum dots formed on Si substrates are attractive for their potential applications as Si-based quantum electronic and photoelectronic devices [1]. For the study of such heteroepitaxial systems, it is essential to investigate the change in the electronic structure due to the strain caused by the lattice mismatch between Si and Ge.

Angle-resolved ultraviolet-photoelectron spectra (ARUPS) of Ge deposited on Si(111) surfaces at $d = 0.1$, 0.5, and 1.0 bilayers (BL, 1 BL corresponds to 1.57×10^{15} atoms/cm^2) have been recorded at BL-7B [2]. The difference ARUPS obtained by subtracting an ARUPS recorded with a clean Si(111)-7×7 surface displays four peaks, as shown in Fig. 5. The three peaks labeled B_1, B_2, and B_3 have been reported as the surface states of the Si(111)-5×5 Ge dimer-adatom-stacking-fault (DAS) structure [3].

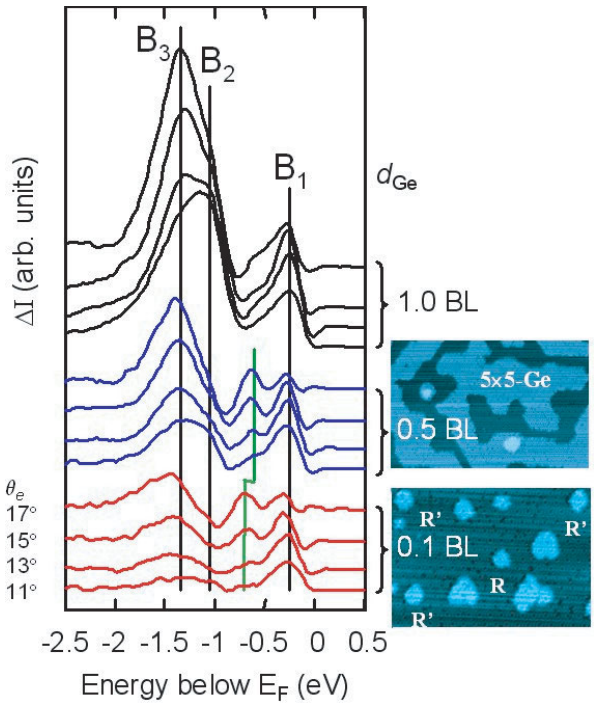

Figure 5
Difference ARUPS of Ge deposited on Si(111) surfaces at $d = 0.1$, 0.5, and 1.0 bilayers obtained by subtracting the ARUPS recorded with a clean Si(111)-7×7 surface. Four spectra, recorded at θ_e = 11°, 13°, 15°, and 17° are plotted for each level of Ge coverage. The positions of the B_1, B_2 and B_3 peaks for the Si(111)-5×5 Ge DAS structure [3] are indicated by solid lines. Also shown are STM images for the $d = 0.1$ BL and $d = 0.5$ BL surfaces.

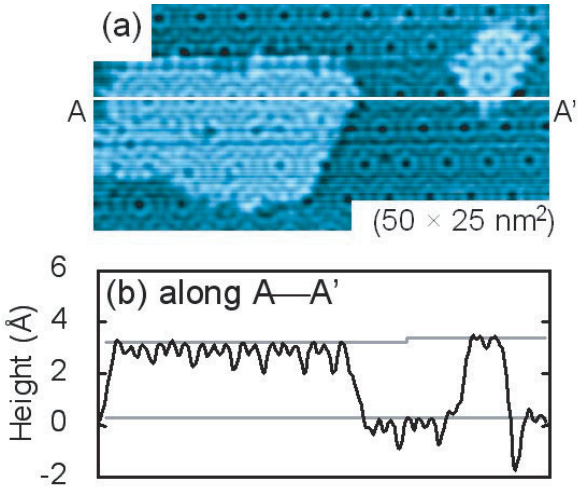

Figure 6
(a) STM image (50 × 25 nm^2) of an area including both small and large Ge islands. (b) Height profile across the adatoms on a small and large island (A-A' line) in (a).

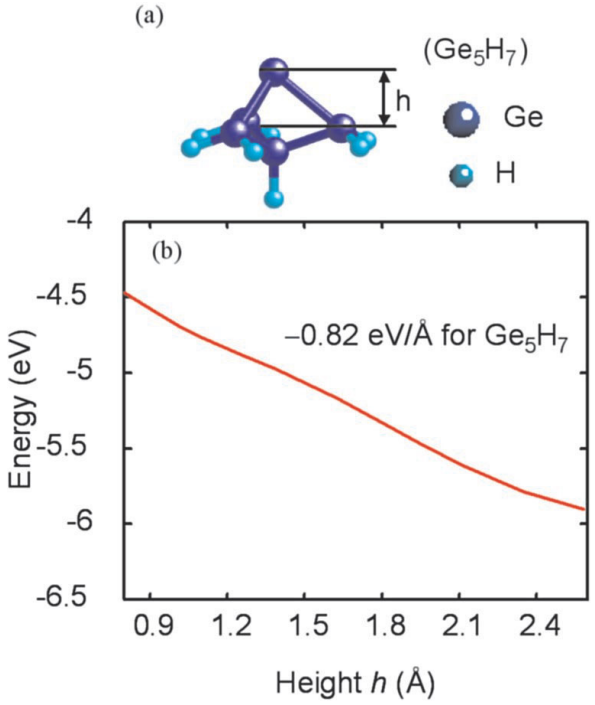

Figure 7
(a) Model cluster energy calculation. The cluster forms a T_4 site and all the Ge atoms except for the adatom were fixed on the ideal sites of the Si bulk crystal. (b) Relationship between the height of the adatom and the energy of the DB state for the Ge clusters.

An additional peak is observed between the B_1 and B_2 peaks. The peak appears at 0.7 eV below the Fermi level even for the low coverage of 0.1 BL, shifting to 0.6 eV at d = 0.5 BL. The peak is hardly observed at d = 1.0 BL, in contrast to the growth of the B_1, B_2 and B_3 peaks. STM images of Ge/Si(111) surfaces at d = 0.1 and 0.5 BL are also shown in Fig. 5. Most of the Ge islands at d = 0.1 BL have small rounded shapes (R) on the surface. The size of the R-islands is about 4 nm but the Ge islands grow up to large sizes at d = 0.5 BL.

We assign the additional peak to the dangling bond (DB) state at the strained adatoms near the edges of the Ge islands as a result of the structural relaxation of the islands for the following reasons [2]: (1) The intensity of the peak is nearly proportional to the total length of the contour line of the Ge first layer composed of islands, that is directly related to the number of adatoms near the edges of the Ge islands; (2) The energy shift is due to difference in strain between the Ge islands having different sizes, since the strain is lower for large islands; (3) The adatom height on the small Ge islands is higher than that on the large islands. Figure 6(a) shows an STM image of small and large Ge islands. The height profile, shown in Fig. 6(b) shows that the adatom height on the small Ge island is ~ 0.01 nm higher than that on the large one. This result is in good agreement with the strain estimated from the ARUPS, since the energy calculation for a cluster forming T_4 sites shows that the energy of the adatom DB state decreases with adatom height almost linearly at –8.2 eV/nm (Fig. 7). This study shows that the strain in the nanoislands can be estimated from the electronic structure at the atomic scale.

M. Suzuki, R. Negishi and Y. Shigeta (Yokohama City Univ.)

References

[1] M. H. Hogen, *Surf. Sci.*, **537** (2003) 1.
[2] M. Suzuki, R. Negishi and Y. Shigeta, *Phys. Rev. B,* **72** (2005) 235325.
[3] P. Mårtensson, W. -X. Ni, G. V. Hansson, J. M. Nicholls and B. Reihl, *Phys. Rev. B,* **36** (1987) 5974.

3-4 Element-Selective Vertical Height Determination of an Organic Monolayer Using a Scanned-Photon-Energy Photoelectron-Yield Soft X-Ray Standing-Wave Technique

Functional organic molecular devices such as liquid-crystal displays, photo-sensitized solar cells and organic electroluminescence devices have been developed using organic thin films. The knowledge of *molecular positions* as well as *molecular alignment* in the films is essential to determine the electronic structure of the films and the dynamic response to external stimuli. Although many techniques are available for obtaining information on molecular alignment, studies of molecular positions in thin films are very limited.

The X-ray standing-wave (SW) technique provides a measure of the location of specific atoms relative to the extended substrate-scatter-plane locations. Since the size of the organic molecules that are actually used for molecular devices is typically several tens of angstroms, it is necessary to generate SWs of long periodicity. For this purpose, we used a multilayer

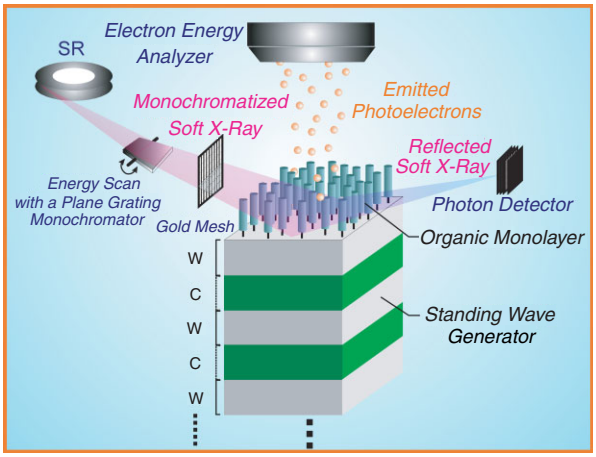

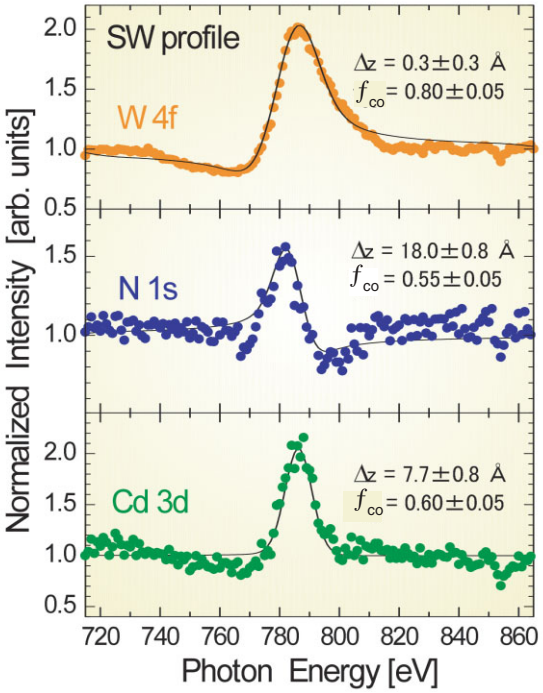

Figure 8
Upper panel: Schematic illustration of the scanned-energy photoelectron-yield soft X-ray standing-wave (SW) measurement for an organic monolayer formed on a SW generator. Lower panel: SW profiles obtained from W-4f, N-1s and Cd-3d XPS peak intensity changes as a function of photon energy (sold circles). The calculated SW profiles using the structural parameters, Δz and f_{co}, are indicated by solid curves.

$(W(12.0\ Å)/C(18.9\ Å))_{80}$ (d = 30.9 Å) and soft X-rays with energies lower than 1 keV (λ ~12 Å). Photoelectron-yield SW-profile measurements with soft X-rays offer high sensitivity to the light elements such as C, N, O and S that are the constituents of organic molecules.

An organic monolayer of the amphiphilic azobenzene derivative $CH_3(CH_2)_7AzO(CH_2)_5COOH$ (Az: $C_6H_5N{=}NC_6H_5$), hereafter denoted by 8Az6, was prepared on the multilayer using the Langmuir-Blodgett (LB) method. Because Cd cations were added into ultra-pure water in the LB method as a stabilizer, the 8Az6 molecules are in the form of Cd-carboxylate. SW profiles were measured at BL-7A by detecting the W-4f, N-1s and Cd-3d photoelectron yield as a function of photon energy at a fixed incident angle of 15° from the surface parallel (Bragg condition: $h\nu$ = 775 eV), as schematically shown in the upper panel of Fig. 8.

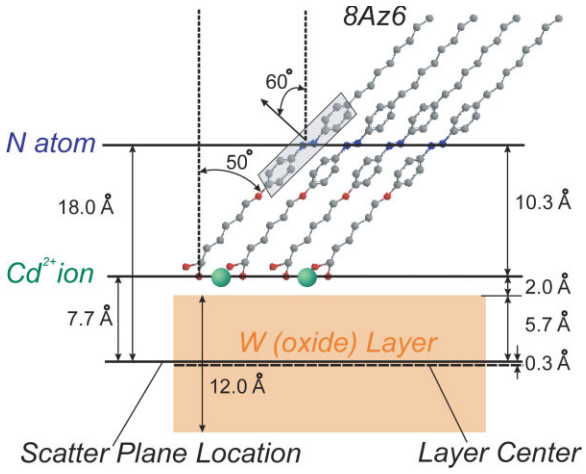

Figure 9
Structure model for the 8Az6-Cd monolayer formed on a $(W/C)_{80}$ multilayer. The height of each element was determined by the present SW technique and the orientation angles were estimated from C-*K* NEXAFS measurements. Note that the surface of the W layer is oxidized, which leads to facile adsorption of Cd-carboxylate to the hydrophilic oxidized surface.

The SW profiles thus obtained are shown in the lower panel of Fig. 8 and exhibit clearly different profiles. A theoretical fit to the SW curves gives different heights (Δz) and coherent factors (f_{co}) for each element, as indicated in the figure. Based on the estimated heights, we propose a structure model for the 8Az6-Cd monolayer as shown in Fig. 9. The X-ray scatter plane is located at almost the center of the 12.0-Å-thick W layer. Cd^{2+} ions were found to be situated just above the W surface, which is quite reasonable if the preparation conditions are taken into account. The N atoms in the Az moiety are located 10.3 Å above the Cd^{2+} layer. C-K NEXAFS measurements indicate that the long molecular axis of 8Az6 in the monolayer is tilted by 50 ± 10° from the surface normal. Assuming that the alkyl chains take the all-trans conformation, the N atoms are expected to be 9.4 ± 2.0 Å above the Cd^{2+} level, consistent with the SW results. Thus, it is demonstrated that this technique is a powerful tool for determining *atomic positions in height* in organic monolayers [1]. Furthermore, the scanned-photon-energy mode enables us to use an ordinary sample manipulator without a precise goniometer and also to upgrade this technique to a fast data-acquisition version by using energy-dispersed X-rays. This will open a way to studying dynamic processes of organic monolayers induced by external stimuli, in particular the relation to vertical height changes.

H. Kondoh[1], R. Yokota[1], K. Amemiya[1], T. Shimada[1], I. Nakai[1], M. Nagasaka[1], T. Nakamura[2], H. Takenaka[3] and T. Ohta[1] ([1]The Univ. of Tokyo, [2]AIST, [3]NTT-AT)

Reference

[1] H. Kondoh, R. Yokota, K. Amemiya, T. Shimada, I. Nakai, M. Nagasaka, T. Ohta, T. Nakamura and H. Takenaka, *Appl. Phys. Lett.*, **87** (2005) 031911.